

SUPPLEMENTAL FIGURES:

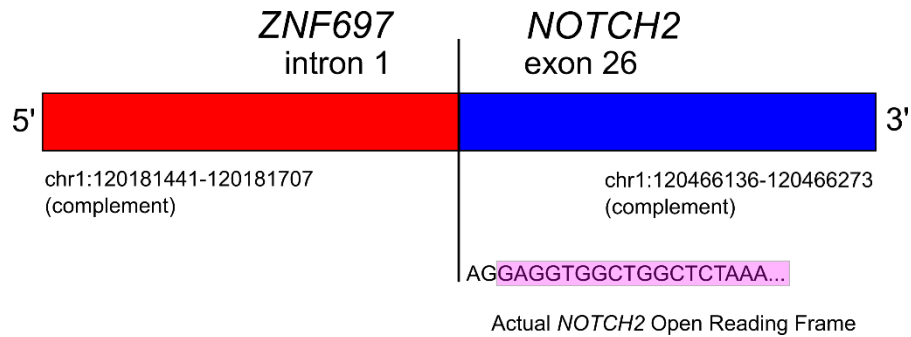


Fig S1. *ZNF697*-*NOTCH2* rearrangement: Diagram of the *ZNF697*-*NOTCH2* fusion and breakpoint. The 5' untranslated region of *ZNF697* is joined out of frame with exon 26 of *NOTCH2*, with the actual reading frame highlighted in pink. Chromosomal coordinates are based on GRCh37/hg19, with genes located on the (-) strand.

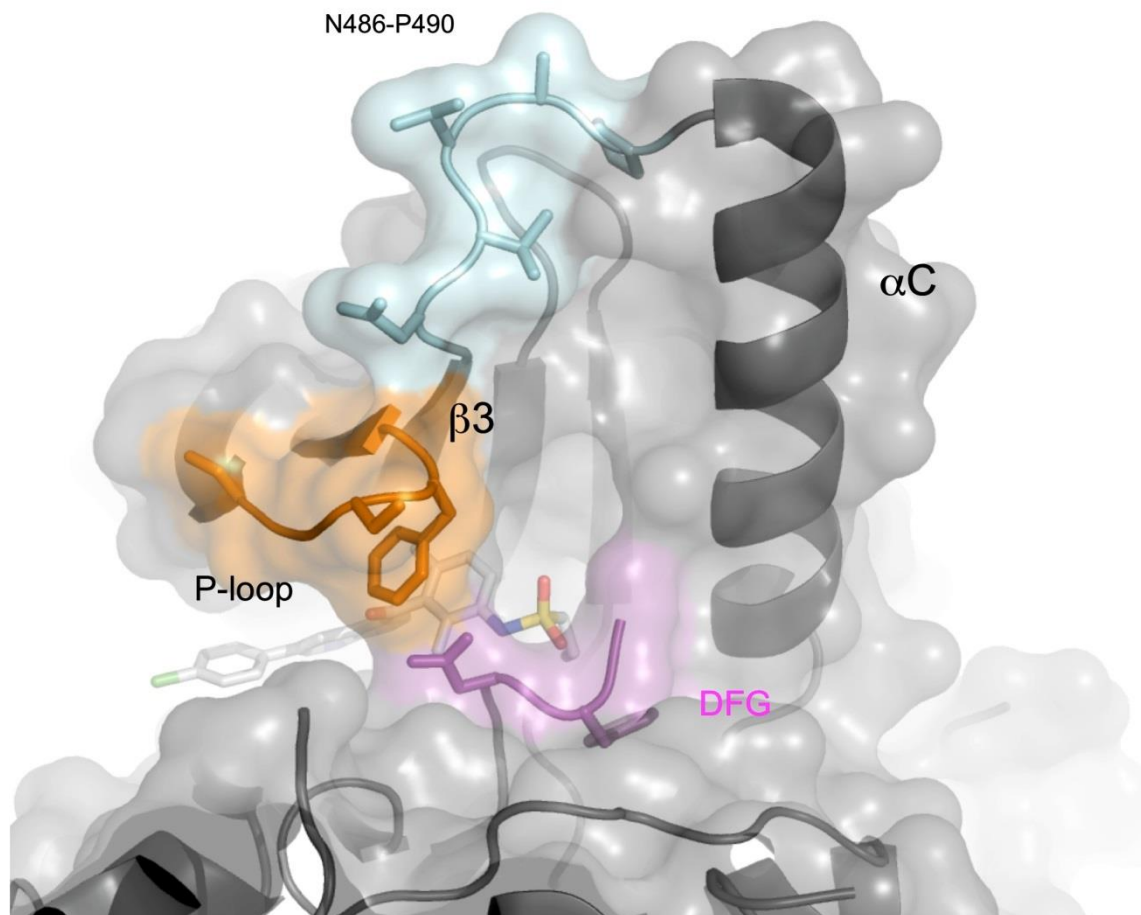


Fig S2. BRAF D486-492 mutation in LCH. Ribbon diagram of the V600E mutant of BRAF kinase domain in complex with the inhibitor Vemurafenib, also known as PLX4032 (PDB ID 3OG7.) (1)The polypeptide Asn486-Pro490 deleted in LCH is in light blue. The DFG motif is in purple. Residues Ser465 to Gly469 of the P-loop are in orange. For simplicity, only side chain residues are shown.

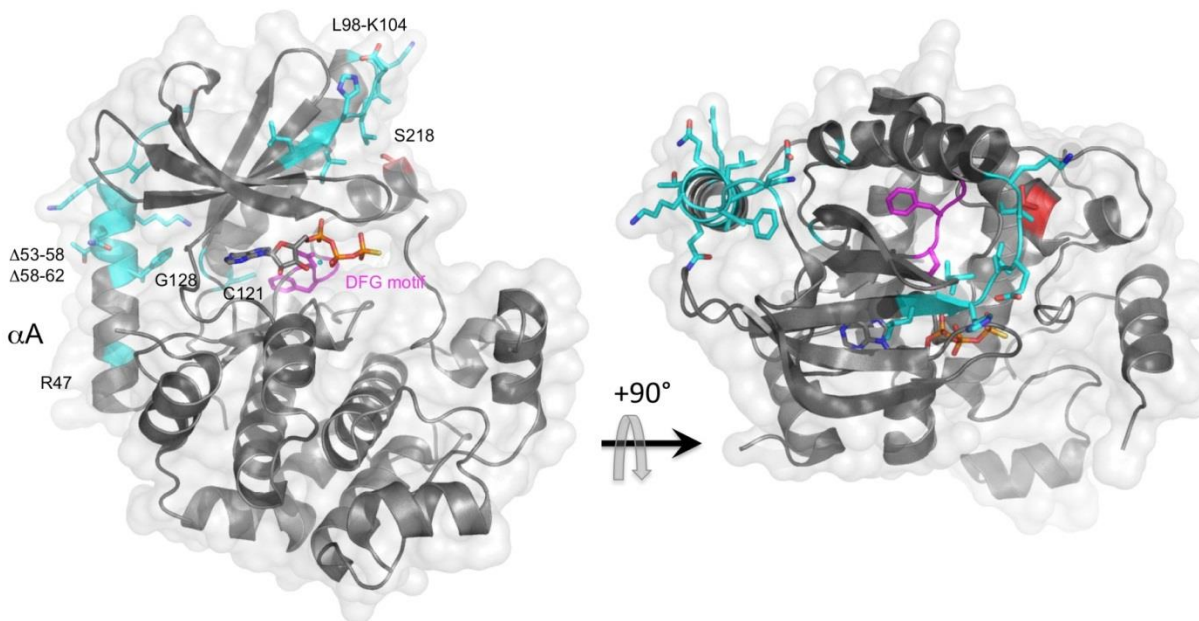


Fig S3. MEK1 mutants in LCH. Ribbon diagram of MEK1 (residues 34-393) in complex with ATP γ S/Mg $^{2+}$ (PDB ID 3QEC) (2). LCH mutations found in this study (F53-Q58>L,Q58-E62del, L98-K104>Q) are indicated in cyan. Also shown are R47, C121 and G128. The ATP γ S and Mg $^{2+}$ -ion are in a ball-and-stick representation. The DFG motif is in pink. Ser218, which is mutated to Asp in the MEK-DD construct, is in red. The two views shown in this figure are at right angles. Only side chains are shown for simplicity.

SUPPLEMENTAL METHODS:

Site-directed Mutagenesis

MEK1 and BRAF mutations were made using Phusion High-Fidelity GC master mix or Q5 High-Fidelity polymerase (New England BioLabs) and mutagenic primers (Integrated DNA Technologies) as listed in *Supplemental Table 1*. Post-PCR parental DNA was digested with DpnI (New England BioLabs) up to overnight. 1 μ L of the resulting reaction was transformed into PX10b (Protein Express, Cincinnati, OH) competent bacteria. Colonies were minipreped (Qiagen) and positive clones were determined by Sanger sequencing through the CCHMC DNA Sequencing and Genotyping core facility.

Retroviral Particle Production and Transduction

Retrovirus was produced by transfecting HEK293T cells with the pBABE-HA-MEK mutant plasmids, pCL-Eco, and M57 helper plasmids. Supernatant was harvested at 24 and 48 hours after transfection, and sterile filtered. NIH/3T3 and BaF/3 cells were transduced by incubating overnight with viral supernatant and polybrene, then subsequently selected with puromycin (3 μ g/mL for NIH/3T3 and 0.5 μ g/mL for BaF/3 cells). All experiments involving recombinant DNA were conducted in accordance with the NIH Guidelines for Research Involving Recombinant or Synthetic Nucleic Acid Molecules. Retroviral production and manipulation was performed in BSL-2 rated facilities in accordance with standard safety procedures.

Western Blotting

Antibodies used were against HA-tag (Pierce cat No. 26183,) GAPDH (GeneTex, GTX627408, 1:5000) phospho-p44/42 MAPK (ERK1/2, CST 4370, 1:2000), total ERK1/2 (CST 4696, 1:2000) and secondary anti-mouse Eu (Molecular Devices R8205) and anti-rabbit Eu (Molecular Devices R8204) antibodies. Lysates were prepared by boiling in RIPA buffer, supplemented with

protease inhibitor (Sigma P8340) and phosphatase inhibitor cocktails (Roche Cat No. 04906845001) for 5-10 minutes, then separated on a 12% SDS-PAGE gel (Bio-Rad). After transfer to a PVDF membrane (Bio-Rad TurboBlot), blots were blocked with 5% (w/v) bovine serum albumin (Fischer Scientific) and incubated overnight with appropriate primary antibodies. Blots were subsequently washed, and probed with the appropriate secondary antibody, then imaged on the SpectraMax i3 platform with the ScanLater module (Molecular Devices.)

In-Cell Western

Following growth and serum starvation, drug treatment with optional EGF stimulation, cells were fixed with 4% formaldehyde (w/v) in Tris-buffered saline, then permeabilized by washing with TBS-Triton X-100 (0.1%). Cells were blocked with TBS-based Odyssey Blocking Buffer (LiCor Biosciences) for one hour, then incubated overnight at 4°C with both primary phospho-p44/42 MAPK (ERK1/2, CST 4370, 1:5000) and total ERK1/2 (CST 4696, 1:5000.) Wells were washed and stained with both secondary antibodies (LiCor Biosciences, IRDye 680 anti-Mouse and IRDye 800 anti-Rabbit, 1:5000) for 1 hour, then washed and scanned on an Odyssey Classic imager using the microplate setting.

Supplementary Table 1: Demographics and clinical features of patient samples submitted for targeted sequencing with identified candidate driver mutations. Alterations represented as amino acid changes, except where indicated.

Case ID	Age	Gender	Diagnosis	Genetic Alterations
A-ECD-1	48	Male	ECD	<i>MDM2</i> amplification
A-ECD-2	77	Female	ECD	<i>BRAF</i> V600E
A-ECD-3	61	Male	ECD	<i>BRAF</i> V600E
A-ECD-7	55	Male	ECD	<i>BRAF</i> V600E
A-NOS-13	63	Female	NOS	<i>ETV3-NCOA2</i> rearrangement
P-JXG-15	1	Male	JXG	<i>CDKN2A/B</i> loss, <i>MAP2K1</i> F53_Q58>del
A-NOS-17	46	Male	NOS	<i>CDK6</i> , <i>EMSY</i> , <i>KIT</i> , <i>MDM2</i> , <i>PDGFRA</i> amplification; <i>ZNF697-NOTCH2</i> rearrangement
A-RDD-20	45	Female	RDD	<i>KRAS</i> K117N
P-LCH-21	18	Female	LCH	<i>BRAF</i> N486_P490del
A-NOS-22	86	Male	NOS	<i>DNMT3A</i> R882C
A-ECD-24	57	Male	ECD	<i>CDKN2A/B</i> loss, <i>MAP3K1</i> amplification, <i>TP53</i> L264del
P-LCH-25	4	Male	LCH	<i>MAP2K1</i> Q58_E62del
P-LCH-27	10	Male	LCH	<i>MAP2K1</i> E102_I103del
P-LCH-28	1	Male	LCH	<i>BRAF</i> V600E
P-NOS-29	13	Female	NOS	<i>EML4-ALK</i> rearrangement
A-ECD-31	43	Male	ECD	<i>NCOR2</i> splice site 1483-4_1496delACAGCAGCAGCAACAACA
A-LCH-32	72	Female	LCH	<i>KRAS</i> Q61H, <i>KRAS</i> amplification, <i>RBM10</i> E47*
A-ECD-33	52	Male	ECD	<i>ASXL1</i> R693*, <i>BRAF</i> V600E, <i>U2AF1</i> Q157P
P-LCH-34	16	Male	LCH	<i>MAP2K1</i> Q58_E62del
P-LCH-35	4	Male	LCH	<i>BRAF</i> V600E
A-ECD-36	55	Male	ECD	<i>MAP2K1</i> Q56P
P-LCH-37	17	Male	LCH	<i>MAP2K1</i> L98_K104>Q
A-RDD-38	58	Male	RDD	<i>CBL</i> C384Y, <i>GNAQ</i> Q209H, <i>KRAS</i> K117N, <i>KRAS</i> A146V
A-NOS-42	40	Female	NOS	<i>BRAF-CLIP2</i> rearrangement
A-LCH-44	65	Male	LCH	<i>TET2</i> H1904R
P-LCH-45	19	Female	LCH	<i>BRAF</i> N486_P490del
A-RDD-46	60	Female	RDD	<i>KRAS</i> K117N
A-ECD-47	63	Female	ECD	<i>ASXL1</i> Q733*, <i>BRAF</i> V600E, <i>NRAS</i> G13D
P-NOS-48	20	Male	NOS	<i>CDKN2A/B</i> loss, <i>NTRK1-TPR</i> rearrangement
P-LCH-50	5	Male	LCH	<i>BRAF</i> V600E
P-JXG-51	1	Female	JXG	<i>KIF5B-ALK</i> rearrangement
A-RDD-52	50	Female	RDD	<i>KDM5A</i> amplification
A-NOS-53	41	Male	NOS	<i>KIF5B-ALK</i> rearrangement
A-LCH-55	56	Female	LCH	<i>BRAF</i> G466R, <i>SRSF2</i> Y44H
A-LCH-56	34	Female	LCH	<i>BRAF</i> V600E
A-LCH-57	56	Female	LCH	<i>BRAF</i> V600E, <i>TET2</i> E1106fs*23, <i>TET2</i> H937fs*16
A-NOS-58	74	Female	NOS	<i>GATA1</i> E13A, <i>MLL2</i> R5432W
P-NOS-59	10	Female	NOS	<i>KIF5B-ALK</i> rearrangement
A-NOS-60	36	Female	NOS	<i>ASXL1</i> Q1063*
A-ECD-61	56	Female	ECD	<i>MAP2K1</i> E102_I103del
P-LCH-62	6	Female	LCH	<i>BRAF</i> N486_T491>K
A-LCH-63	47	Female	LCH	<i>BRAF</i> N486_P490del, <i>DNMT3A</i> Y533C

A-LCH-64	78	Male	LCH	<i>BIRC3</i> S116*, <i>CDKN2A/B</i> loss, <i>FAS</i> loss, <i>KRAS</i> K117N, <i>SETD2</i> splice site 7431+2_7431+24del23
P-LCH-65	11	Female	LCH	<i>MAP2K1</i> E102_I103del
P-LCH-66	8	Male	LCH	<i>BRCA1</i> splice site 536_547+165del177, <i>MAP2K1</i> Q58_E62del
A-ECD-68	60	Male	ECD	<i>ASXL1</i> E635fs*15, <i>BRAF</i> V600E
A-LCH-69	34	Male	LCH	<i>BRAF</i> V600E
A-LCH-71	57	Female	LCH	<i>BRAF</i> V600E, <i>KRAS</i> G13C, <i>NRAS</i> G12D
A-RDD-73	29	Female	RDD	<i>FBXW7</i> E113D
A-LCH-74	52	Female	LCH	<i>ETV3-NCOA2</i> rearrangement
A-ECD-79	45	Female	ECD	<i>BRAF</i> V600E
A-ECD-81	56	Female	ECD	<i>MAP2K1</i> F53L
A-LCH-82	50	Male	LCH	<i>GNAS</i> R201C
P-LCH-83	2	Female	LCH	<i>BRAF</i> V600E
P-LCH-84	2	Male	LCH	<i>MAP2K1</i> Q56_G61>R
A-NOS-85	78	Male	NOS	<i>NOTCH1</i> E450K, <i>SRSF2</i> P95R

Supplementary Table 2: Characteristics of patients for whom no candidate driver mutations were identified by sequencing

Age	Gender	Disease
53	Female	ECD
29	Female	ECD
<1	Male	JXG
4	Female	LCH
1	Male	LCH
49	Male	NOS
14	Female	NOS
6	Male	NOS
56	Male	NOS
47	Male	NOS
16	Female	RDD
21	Female	RDD
15	Male	RDD
71	Female	RDD
57	Female	RDD
44	Male	RDD

Supplementary Table 3: Mutagenic PCR Primers used to generate *MAP2K1* mutations.

Gene	Mutation	Primer	Sequence
<i>MAP2K1</i>	R47Q	Forward	GCCTCAAGGCGCTTTTGCTGCTGCTCATCAA
<i>MAP2K1</i>	R47Q	Reverse	TTGATGAGCAGCAGCAAAAGCGCCTTGAGGC
<i>MAP2K1</i>	F53_Q58>L	Forward	GCGCCTTGAGGCCTTGAAGGTGGGAGAACT
<i>MAP2K1</i>	F53_Q58>L	Reverse	AGTTCTCCACCTTCAAGGCCTCAAGGCGC
<i>MAP2K1</i>	Q58_E62del	Forward	GCCTTTCTTACCCAGAAGCTGAAGGATGACGACTTT
<i>MAP2K1</i>	Q58_E62del	Reverse	AAAGTCGTCATCCTTCAGCTTCTGGGTAAGAAAGGC
<i>MAP2K1</i>	E102_I103del	Forward	CAGAAAGCTAATTCATCTGAAACCCGCAATCCGGAAC

<i>MAP2K1</i>	E102_I103del	Reverse	GTTCCGGATTGCGGGTTTCAGATGAATTAGCTTTCTG
<i>MAP2K1</i>	C121S	Forward	ATGTACGGAGAGTTGCTCTCATGCAGAACCTGC
<i>MAP2K1</i>	C121S	Reverse	GCAGGTTCTGCATGAGAGCAACTCTCCGTACAT
<i>MAP2K1</i>	G128V	Forward	GAACGCACCATAGAAGACCACGATGTACGGAGA
<i>MAP2K1</i>	G128V	Reverse	TCTCCGTACATCGTGGTCTTCTATGGTGCGTTC

Supplementary References:

1. Bollag G, Hirth P, Tsai J, Zhang J, Ibrahim PN, Cho H, Spevak W, Zhang C, Zhang Y, Habets G, et al. Clinical efficacy of a RAF inhibitor needs broad target blockade in BRAF-mutant melanoma. *Nature*. 2010;467(7315):596-9.
2. Fischmann TO, Smith CK, Mayhood TW, Myers JE, Reichert P, Mannarino A, Carr D, Zhu H, Wong J, Yang RS, et al. Crystal structures of MEK1 binary and ternary complexes with nucleotides and inhibitors. *Biochemistry*. 2009;48(12):2661-74.